IJEEC

International Journal of Electrical Engineering and Computing
Vol. 5, No. 2 (2021)

Original research paper
UDC 621.38:[681.586:621.317.38
DOI 10.7251/IJEEC2102069K

Approximate Magnetic Flux Density Model of Overhead Power Lines for Conductor Sag Estimation

Nemanja Kitić and Petar Matić

Faculty of Electrical Engineering, University of Banja Luka, Banja Luka, Republic of Srpska, Bosnia and Herzegovina

E-mail address: nemanja.kitic@etf.unibl.org, petar.matic@etf.unibl.org

Abstract—**Monitoring and supervision of overhead power lines have become essential actions in Electrical Power Systems since the introduction of the Smart Grid concept. In order to monitor overhead power lines, simple non-invasive devices are mounted on support poles, which detect line abnormalities and faults by measuring magnetic field originating from power line conductors. Measured signals are also used to determine various electrical and non-electrical line parameters. In this paper a new approximate model for magnetic flux density vector components of the overhead power lines suitable for real-time conductor sag estimation is presented. In the proposed model, catenary-shaped power line conductors are approximated with tilted straight line conductors, and the approximate model is calibrated by tuning model coefficients to match flux density vector components as in the case of real catenary-shaped conductors. The accuracy of the proposed model is verified by measurements on three-phase overhead power line model scaled to laboratory conditions. As a conclusion, an adaptive method for possible practical implementation based on the approximate model is considered.**

Keywords - Fault Passage Indicator; Magnetic Flux Density; Overhead Power Line; Sag;

I. INTRODUCTION

The key factor for proper and safe operation of Electrical Power System (EPS) is monitoring and supervision of overhead power lines. In contemporary EPS, since introduction of Smart Grid concept, it is common to use non-contact devices which measure magnetic flux density components in the vicinity of power line conductors [1]. These devices are used for monitoring line status during normal operation and acquiring information about abnormal regimes, like faults [2]. Beside their main function, these devices could be used for estimation of other electrical and non-electrical parameters of overhead lines (OHL), like conductor sag [3].

Accurate information about conductor sag is necessary due to safety reasons related to minimum ground clearance, but the sag also affects line transmission capabilities by limiting line current capacity. Conductor sag depends both on line current (conductor heating because of resistive losses) and ambient conditions (outdoor temperature, wind, snow and ice on the conductors). Even though the maximum value of conductor sag should be already taken into account during the design phase, the actual value of conductor sag should also be monitored and accounted for.

There are several methods for sag determination, based on measuring physical line parameters (distance, temperature, vibrations, tension) or using different measurement techniques and signal processing (special sensors, image processing, etc) [4]. In [5] a method for sag monitoring by measuring induced current in high resistive wire attached on transmission line towers was proposed. A method for conductor sag measurement using differential GPS was proposed in [6], but it is impractical due to complex algorithm for sag calculation and issues related to GPS sensor mounting. However, the most of contemporary techniques for accurate sag estimation require complex models and use of non-conventional sensors, which are sensitive to ambient conditions, and in general are expensive, non-convenient for mass use for transmission and distribution OHL.

In this paper an approximate magnetic flux density model of OHL for simple and inexpensive power line sag monitoring method is proposed. The method is based on processing the signals from Fault Passage Indicators (FPI) which are widely used as devices for contactless fault detection in EPS. Those devices are mounted on suitable support poles or towers underneath overhead power line conductors, and by measuring conductor magnetic flux density they can detect the passage of fault current through power line conductors [2]. Since the information about magnetic flux density components and line current is already available in those devices, their software can be upgraded to monitor conductor sag. However, calculation of conductor sag from measured line currents and magnetic flux density is a complicated task due to complexity of mathematical model which correlates line geometry, currents and magnetic flux density. Thus, for accurate conductor sag calculation in inexpensive devices like FPIs, a simplified power line magnetic flux density model should be derived, which is the main subject of this paper.

This paper has been financially supported in part by the Ministry for Scientific and Technological Development, Higher Education and Information Society of the Republic of Srpska under the project Fault detection on overhead distribution power lines based on contactless magnetic field measurement.

The paper is organized as follows. Section II is related to modeling three-phase overhead power line based on general mathematical model well known from the very early studies [7]. Since the magnetic flux density vector of catenary-shaped conductor cannot be calculated in closed form, in Section III an approximation for magnetic field spatial distribution, valid in the vicinity of the conductor suspension points (the place where the sensor is mounted) will be proposed. In Section IV the proposed approximate model will be calibrated to match the general model by tuning model coefficients. The accuracy of the approximate model will be confirmed in Section V, in which the proposed model will be tested by set of experiments on a three-phase power line model scaled to laboratory conditions. Section VI is a conclusion, in which some remarks about practical implementation will be given.

II. General Model for Magnetic Flux Density of Overhead Power Lines

In this Section an overview of basic equations and general application of Biot-Savart law for catenary-shaped overhead power lines will be shortly overviewed, as a basis and reference model for subsequent analysis.

Biot-Savart law for magnetic flux density vector of a single current-carrying conductor in free space at given point is represented by [7]:

$$\underline{\mathbf{B}} = \int_L \frac{\mu_0}{4\pi} \cdot \frac{\left(\underline{\mathbf{I}} \cdot \overrightarrow{dl}\right) \times \vec{a}_0}{|\vec{r}|^2}, \tag{1}$$

where L is overall conductor length, $\mu_0 = 4\pi \times 10^{-7}$ H/m is the magnetic permeability of free space, $\underline{\mathbf{I}}$ is the complex current, $\overrightarrow{dl}$ is differential element of length at direction of the current, $\vec{r}$ is the position vector from differential element $\overrightarrow{dl}$ to the given point, $\vec{a}_0$ is the unit vector with direction same as $\vec{r}$.

General model for spatial distribution of real power line magnetic field must take into account the catenary shape of conductors which are suspended between supporting poles or towers. Fig. 1a illustrates two symmetrical spans of three-phase power line catenary-shaped conductors, with the same distance $y_j(0)$ to the reference coordinate system origin in y-axis direction and distance between poles marked as L. The origin of the reference coordinate system is at the middle pole where the monitoring sensor is mounted. The sag of the conductors s is measured at the midspan, from horizontal line that connects suspension points of the conductors to the lowest height of the conductors. Catenary or chain curve is expressed as [2]:

$$y_j(z) = a \cdot \left[\cosh\left(\frac{2 \cdot z - \mathrm{sign}(z) L}{2 \cdot a} \right) - 1 \right] + y_j(0) - s, \tag{2}$$

where, a is catenary parameter defined as $a = L^2/(8 \cdot s)$.

For the three-phase power system, overall magnetic field measured at the origin is the result of all three catenary-shaped current-carrying conductors. Magnetic flux density vector components take into account different current amplitudes and phase angles of each phase, in conjunction with geometry of the conductors at the suspension points as illustrated in Fig. 1b. The resulting magnetic flux density vector components of three-phase catenary-shaped overhead power line, expressed in the sensor reference coordinate system, are [7]:

$$\underline{\mathbf{B}}_x = \sum_{j=\mathrm{A,B,C}} \frac{\mu_0 \cdot \underline{\mathbf{I}}_j}{4\pi} \int_{-L}^{L} \frac{y_j(z) - z \cdot \sinh\left[\dfrac{2 \cdot z - \mathrm{sign}(z) L}{2 \cdot a} \right]}{\left[x_j^2 + y_j^2(z) + z^2 \right]^{3/2}} dz, \tag{3}$$

$$\underline{\mathbf{B}}_y = \sum_{j=\mathrm{A,B,C}} \frac{\mu_0 \cdot \underline{\mathbf{I}}_j}{4\pi} \int_{-L}^{L} \frac{-x_j}{\left[x_j^2 + y_j^2(z) + z^2 \right]^{3/2}} dz, \tag{4}$$

$$\underline{\mathbf{B}}_z = \sum_{j=\mathrm{A,B,C}} \frac{\mu_0 \cdot \underline{\mathbf{I}}_j}{4\pi} \int_{-L}^{L} \frac{x_j \cdot \sinh\left(\dfrac{2 \cdot z - \mathrm{sign}(z) L}{2 \cdot a} \right)}{\left[x_j^2 + y_j^2(z) + z^2 \right]^{3/2}} dz, \tag{5}$$

where, x_j and y_j are coordinates of conductor j, and $\underline{\mathbf{I}}_j$ are the complex phase currents, j = A, B, C. In the model, ground return current is neglected since its contribution to the magnetic field is low and not notable in the vicinity of the power conductors, where the magnetic sensor is placed and where catenary effects are only notable [7].

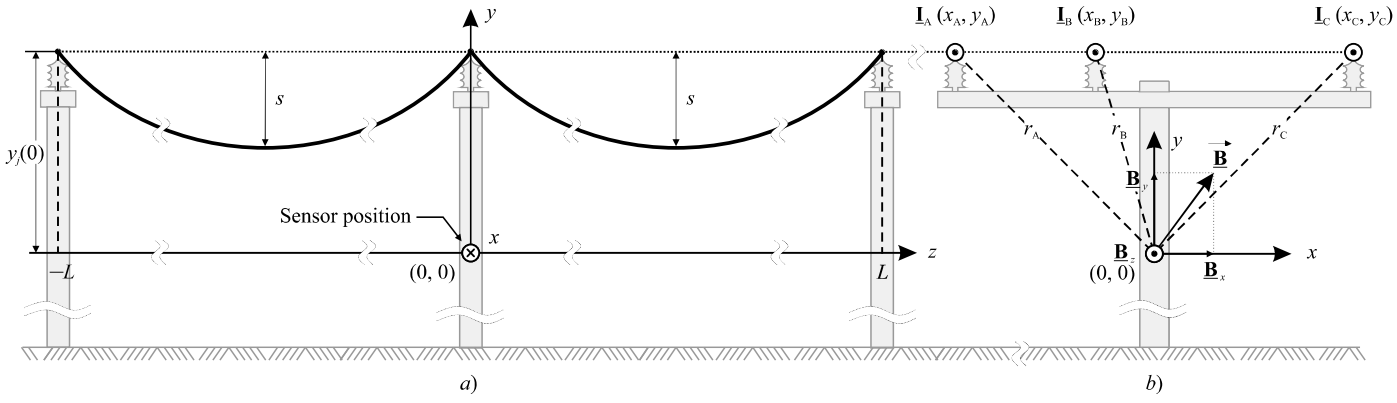

Figure 1. Two symmetrical spans of three-phase power line with sensor placed on the middle pole as a coordinate system origin: a) side view, b) front view

III. Approximate Model for Magnetic Flux Density of Overhead Power Lines

Magnetic flux density vector components given by reference model (3)–(5) cannot be solved analytically [7], and only can be solved by numerical integration, which is unsuitable for real-time application in cheap devices for conductor sag estimation in EPS. For that reason, an approximation which will provide closed form solution of (3)–(5) is proposed in this Section. First, a single catenary-shaped conductor is considered, and after that, a three-phase catenary-shaped power line of given geometry.

A. Approximation of single catenary-shaped conductor

Closed form solution of the Biot-Savart law (1) can be found for a straight line current-carrying conductor which is in the same plane as the origin of the coordinate system (i.e. the system of conductor and the origin is coplanar), as shown in Fig 2. Intensity of magnetic flux density vector is [8]:

$$\underline{\mathbf{B}} = \frac{\mu_0 \cdot \underline{\mathbf{I}}}{4\pi \cdot r}\left(\sin\theta_2 - \sin\theta_1\right), \tag{6}$$

where $r = y(0)$ is normal distance from conductor to the origin of coordinate system. Angles θ_1 and θ_2 in (6) depend on conductor length L, normal distance r and are indicated in Fig. 2, while direction of the magnetic flux density vector $\underline{\mathbf{B}}$ is determined by the right-hand rule.

In order to take into account power line conductor sag and to maintain closed form solution of Biot-Savart integral, catenary-shaped conductors will be approximated with the tilted straight half-lines of infinite length as shown in Fig. 3. This approximation is valid close to the suspension points and also where magnetic field sensor is placed.

In Fig. 3 the origin of the reference coordinate system is in a straight line below conductor suspension point and therefore is coplanar with the conductor. The intensity of magnetic flux density vector of conductor is calculated by (6), by dividing it into two half-lines starting at suspension point, which create two segments, S1 (left) and S2 (right). Those half-lines are symmetrical (mirrored image of each other), and the intensity of magnetic flux density of segment S1 is found by one half-line of infinite length from (6) as:

$$\begin{aligned}\underline{\mathbf{B}}_{tilted,\mathrm{S1}} &= \frac{\mu_0 \cdot \underline{\mathbf{I}}}{4\pi \cdot y(0)\cdot\cos(\alpha)}\left[\sin(\alpha) - \sin\left(-\frac{\pi}{2}\right)\right] = \\ &= \frac{\mu_0 \cdot \underline{\mathbf{I}}}{4\pi \cdot y(0)\cdot\cos(\alpha)}\left[\sin(\alpha)+1\right]\end{aligned}, \tag{7}$$

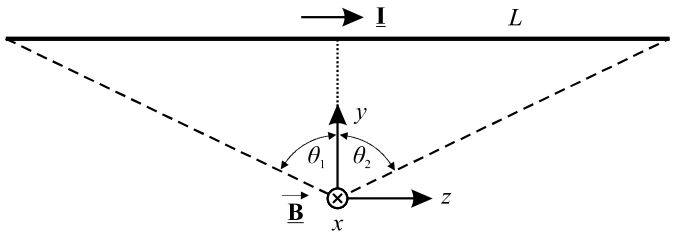

Figure 2. Basic application of Biot-Savart law

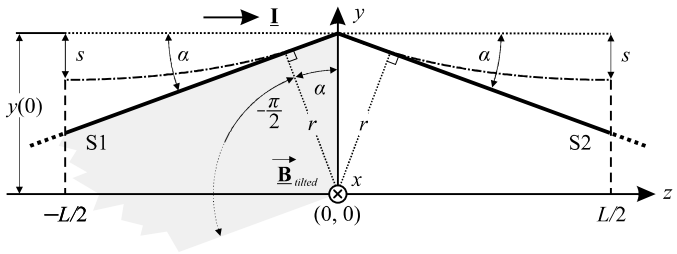

Figure 3. Current-carrying conductor approximated with tilted straight line

with $\theta_1 = -\pi/2$ and $\theta_2 = \alpha$, and normal distance between conductor and coordinate system origin is $r = y(0)\cdot\cos(\alpha)$. Direction of the magnetic flux density vector $\underline{\mathbf{B}}_{tilted,\mathrm{S1}}$ is determined by the right-hand rule and it is perpendicular to the plane formed by the conductor and origin. Overall magnetic field of both segments, which are both coplanar with the sensor, using symmetry, is $\underline{\mathbf{B}}_{tilted} = 2\cdot\underline{\mathbf{B}}_{tilted,\mathrm{S1}}$. Magnetic flux density vector in (7) is calculated in a closed form, and depends on the angle α which is a function of the sag.

B. Approximation of three-phase catenary-shaped power line

For the case of three-phase overhead power line with geometry of support pole from Fig. 1b, similar approximation with straight half-line conductors can be made. In this case, due to pole geometry, phase conductors in left and right segments are not coplanar with the sensor, and each half-line must be considered separately, having in total 6 different segments for three phases. This is shown in Fig. 4, for a given pole geometry, where each of the half-lines with the origin forms one coplanar segment. Pairs of segments S1-S2 are created by phase A, S3-S4 by phase B, and S5-S6 by phase C. Magnetic flux density vector of each segment is perpendicular to the plane of that segment, with direction determined by right-hand rule and its intensity can be calculated using (6).

The resulting magnetic flux density vector in sensor *xyz* coordinate system can be found by using principle of superposition. Magnetic flux density vector of each segment $n = 1,2..6$ is decomposed to the components projected in sensor reference coordinate system and individual components are added. In Fig. 5 simplified illustration of n-th segment is depicted, where all lengths and angles for magnetic flux density vector decomposition are indicated. As it can be seen from Fig. 5, magnetic flux density vector from n-th segment $\underline{\mathbf{B}}^n_{xyz}$ has three components of magnetic flux density ($\underline{\mathbf{B}}^n_x$, $\underline{\mathbf{B}}^n_y$ and $\underline{\mathbf{B}}^n_z$) which should be calculated.

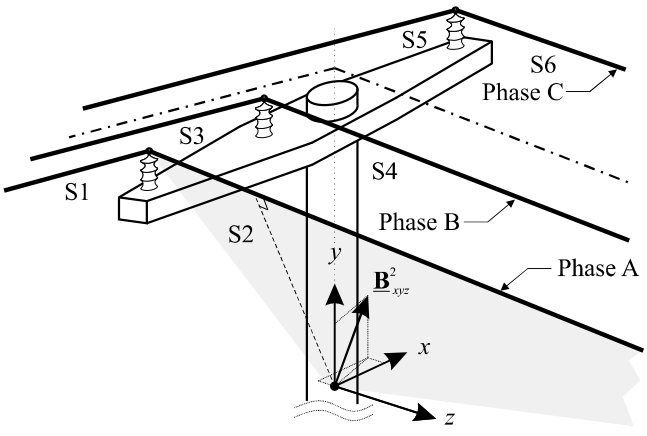

Figure 4. Segments S1 to S6 for three-phase overhead power line

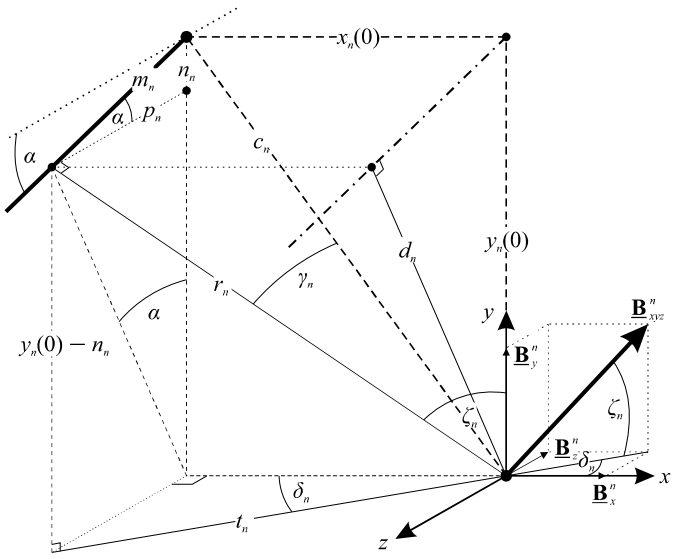

Figure 5. Simplified illustration of *n*-th segment of overhead power line

For *n*-th segment, distances $x_n(0)$ and $y_n(0)$, defined by the pole geometry, are input variables, while the angle α depends on conductor sag. From Fig. 5 normal distance between current-carrying conductor and origin is:

$$r_n = \sqrt{x_n(0)^2 + {d_n}^2}\ ,\ d_n = y_n(0)\cdot\cos(\alpha). \tag{8}$$

The angles in (6) are $\theta_1 = -\pi/2$ and $\theta_2 = \gamma_n$ and sine value of angle γ_n is given by:

$$\sin(\gamma_n) = \frac{m_n}{c_n}, \tag{9}$$

with c_n and m_n:

$$c_n = \sqrt{x_n(0)^2 + y_n(0)^2}, m_n = \sqrt{{c_n}^2 - {r_n}^2} = y_n(0)\cdot\sin(\alpha). \tag{10}$$

The normal distance of current-carrying conductor from the origin r_n, can be expressed as function of known variables by substituting d_n from (8):

$$r_n = \sqrt{x_n(0)^2 + \left[y_n(0)\cdot\cos(\alpha)\right]^2}\ , \tag{11}$$

as well as, sine value of the angle γ_n, which is obtained by substituting (10) into (9):

$$\sin(\gamma_n) = \frac{y_n(0)\cdot\sin(\alpha)}{\sqrt{x_n(0)^2 + y_n(0)^2}}. \tag{12}$$

The intensity of the magnetic flux density vector for *n*-th segment is expressed in the function of known variables by substituting (11) and (12) into (6) as:

$$\underline{\mathbf{B}}^n_{xyz} = \frac{\mu_0\cdot\underline{\mathbf{I}}_n}{4\pi\cdot r_n}\left[\sin(\gamma_n)+1\right], \tag{13}$$

and its projections on *x*, *y* and *z*-axis of the reference coordinate system can be found. From Fig. 5 those projections are:

$$\begin{aligned}\underline{\mathbf{B}}^n_x &= \underline{\mathbf{B}}^n_{xyz}\cdot\cos(\zeta_n)\cdot\cos(\delta_n),\\ \underline{\mathbf{B}}^n_y &= \underline{\mathbf{B}}^n_{xyz}\cdot\sin(\zeta_n),\\ \underline{\mathbf{B}}^n_z &= \underline{\mathbf{B}}^n_{xyz}\cdot\cos(\zeta_n)\cdot\sin(\delta_n),\end{aligned} \tag{14}$$

where sine and cosine of the angles ζ_n and δ_n can be found also from Fig 5. Since the magnetic flux density vector (13) creates the same angle ζ_n with the *xz*-plane as the angle between normal distance r_n and *y*-axis, sine and cosine values of angle ζ_n can be found from:

$$\sin(\zeta_n) = \frac{t_n}{r_n},\quad \cos(\zeta_n) = \frac{y_n(0) - n_n}{r_n}, \tag{15}$$

while the sine and cosine values of angle δ_n are determined by the projection of the normal distance r_n to the *xz*-plane and negative *x*-axis as:

$$\sin(\delta_n) = \frac{p_n}{t_n},\quad \cos(\delta_n) = \frac{x_n(0)}{t_n}. \tag{16}$$

Lengths t_n, n_n and p_n are calculated as:

$$n_n = m_n\cdot\sin(\alpha),\ t_n = \sqrt{x_n(0)^2 + {p_n}^2},\ p_n = m_n\cdot\cos(\alpha), \tag{17}$$

and by substituting (11) and (17) into (15) and (16), sine and cosine values expressed as functions of known variables are:

$$\sin(\zeta_n) = \frac{\sqrt{x_n(0)^2 + \left[y_n(0)\cdot\cos(\alpha)\cdot\sin(\alpha)\right]^2}}{\sqrt{x_n(0)^2 + \left[y_n(0)\cdot\cos(\alpha)\right]^2}}, \tag{18}$$

$$\cos(\zeta_n) = \frac{y_n(0) - y_n(0)\cdot\sin^2(\alpha)}{\sqrt{x_n(0)^2 + \left[y_n(0)\cdot\cos(\alpha)\right]^2}}, \tag{19}$$

$$\sin(\delta_n) = \frac{y_n(0)\cdot\sin(2\cdot\alpha)}{2\cdot\sqrt{x_n(0)^2 + \frac{1}{4}\left[y_n(0)\cdot\sin(2\cdot\alpha)\right]^2}}, \tag{20}$$

$$\cos(\delta_n) = \frac{x_n(0)}{\sqrt{x_n(0)^2 + \left[y_n(0)\cdot\cos(\alpha)\cdot\sin(\alpha)\right]^2}}. \tag{21}$$

The resulting magnetic flux density vector components for three-phase power line are obtained using principle of superposition by adding the components (14) from all six segments. Since conductors for phases A and B in Fig. 4 are placed on the left hand side to reference *xyz* system, the *x*-components of segments S1-S4 for phases A and B are positive, while for the segments S5-S6 of phase C are negative. Similarly, *y*-components of segments S1-S4 for phases A and B are positive, while for the segments S5-S6 of phase C are negative, while, due to symmetry, resulting *z*-component will be zero:

$$\underline{\mathbf{B}}_{x,approx.} = \sum_{n=1}^{4}\left\{\frac{\mu_0\cdot\underline{\mathbf{I}}_n}{4\pi\cdot r_n}\left[\sin(\gamma_n)+1\right]\cos(\zeta_n)\cos(\delta_n)\right\}+ -\sum_{n=5}^{6}\left\{\frac{\mu_0\cdot\underline{\mathbf{I}}_n}{4\pi\cdot r_n}\left[\sin(\gamma_n)+1\right]\cos(\zeta_n)\cos(\delta_n)\right\} \quad (22)$$

$$\underline{\mathbf{B}}_{y,approx.} = \sum_{n=1}^{4}\left\{\frac{\mu_0\cdot\underline{\mathbf{I}}_n}{4\pi\cdot r_n}\left[\sin(\gamma_n)+1\right]\sin(\zeta_n)\right\}+ -\sum_{n=5}^{6}\left\{\frac{\mu_0\cdot\underline{\mathbf{I}}_n}{4\pi\cdot r_n}\left[\sin(\gamma_n)+1\right]\sin(\zeta_n)\right\}, \quad (23)$$

$$\underline{\mathbf{B}}_{z,approx.} = 0\,. \quad (24)$$

In (22)–(24) current $\underline{\mathbf{I}}_n$ is equal to $\underline{\mathbf{I}}_A$ for n=1,2, $\underline{\mathbf{I}}_B$ for n=3,4 and $\underline{\mathbf{I}}_C$ for n=5,6 since the phase currents are the same for pairs of segments S1-S2, S3-S4 and S5-S6.

IV. Calibration of Approximate Model

The approximate model of overhead power line (22)–(24) with conductor sag taken into account is solved in a closed analytical form instead of reference model (3)–(5). The approximate magnetic flux density vector components are functions of phase currents, geometry of the support pole, and the angle α in the model as the multivariate function of catenary sag and conductor span. This function will be analyzed in more detail in this Section in order to provide satisfying accuracy of the approximate model.

The angle α of approximate tilted straight line conductor in each segment from Figs. 3 and 4 can be expressed as function:

$$\alpha = g(f, s, L)\,, \quad (25)$$

where f is fixed longitudinal tuning parameter given relatively to power line span L and real catenary sag s. The parameter f will be used as a tuning variable by which approximate model (22)–(24) should have equal outputs as the reference model (3)–(5). By this, approximate model will be calibrated to match the reference through an adequate function between the sag and angle α (25).

Fig. 6 shows a straight line conductor tilted by the angle α and is valid for any one of six segments from Fig. 4.

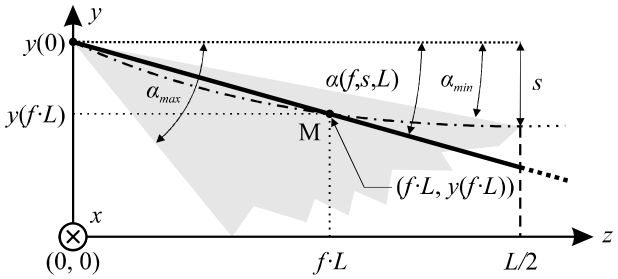

Figure 6. The range of angle α, and relative longitudinal tuning parameter f

For given sag the angle α could range from minimum value α_{min} (for the line that connects suspension point and point with maximum sag), to maximal value α_{max} (for tangent line of catenary in suspension point). By taking into account catenary-shaped curve (2), the slope of tilted straight line conductor from Fig. 6 can be expressed as:

$$k = \frac{y(f\cdot L)-y(0)}{f\cdot L} = \frac{a\cdot\left[\cosh\left(\frac{f\cdot L-0{,}5\cdot L}{a}\right)-1\right]-s}{f\cdot L}, \quad (26)$$

with the parameter f as relative length of the span and $a = L^2/(8\cdot s)$. Parameter f determines the intersection point M($f\cdot L$, $y(f\cdot L)$) of the catenary-shaped and tilted straight line conductor, and it will be chosen in order to match the outputs of the approximate and reference models. Using (26), a relation between angle α and sag s (25) can be expressed in form:

$$\alpha = \tan^{-1}\left\{\frac{L^2 - L^2\cdot\cosh\left[\frac{4\cdot s\cdot(2\cdot f-1)}{L}\right]+8\cdot s^2}{8\cdot f\cdot L\cdot s}\right\}, \quad (27)$$

The best value of tuning parameter f will be determined by comparing magnetic flux densities calculated from approximated model (22)–(23) with values from numerically solved reference model (3)–(4). For calibration purposes tuning parameter f is varied in range (0, 0.5], where starting value corresponds to the tangent line of catenary in suspension point (or to the angle α_{max} in Fig. 6), while end value 0.5 corresponds to the tilted line that connects suspension point and the point with maximum sag (or to the angle α_{min} in Fig. 6).

Percentage errors of the RMS values in x and y components of approximate model are calculated for the range of values of longitudinal parameter f and conductor sag s as:

$$e_x(f,s) = \frac{B_{x,approx.}(f,s)-B_x(s)}{B_x(s)}\cdot 100, \qquad e_y(f,s) = \frac{B_{y,approx.}(f,s)-B_y(s)}{B_y(s)}\cdot 100, \quad (28)$$

where $B_{x,approx.}$ and $B_{y,approx.}$ are RMS values of magnetic flux density components of approximate model (22)–(23), while B_x

and B_y are RMS values of magnetic flux density components of general reference model (3)–(4). Standard deviations of approximate magnetic flux density components are calculated for each pair of longitudinal parameter f and conductor sag s by equations:

$$\sigma_x = \sqrt{\frac{1}{N}\sum_i \left[B_x^i(s_i) - B_{x,approx.}^i(f_i, s_i) \right]^2},$$
$$\sigma_y = \sqrt{\frac{1}{N}\sum_i \left[B_y^i(s_i) - B_{y,approx.}^i(f_i, s_i) \right]^2}, \quad (29)$$

where N is the number of points in which the calculation was performed.

Calibration is performed by simulating standard 20 kV overhead power line from [9] with geometry of the support pole illustrated on Fig. 1b. In order to validate the model for large ranges of conductor sags, span length in simulations is set to $L = 100$ m, while the sag s is in range from 0 (for the straight line conductor) to 4 m. Calculated errors (28) for x and y magnetic flux density vector components are shown in Fig. 7 and Fig. 8, while standard deviations (29) are shown in Fig. 9 and Fig. 10.

From Fig. 7 it is clear that x component has significant error for large sag values, which cannot be compensated by tuning parameter f. On the other hand, from Fig. 8 it is clear that the error in y component ranges from -2.95% to $+4\%$ for whole sag range and highly depends on tuning parameter f. This means that the proposed approximation is not accurate for modeling x component, but it is very accurate in modeling y component of magnetic flux density. This can be also confirmed by observing standard deviations in Fig. 9 and Fig. 10, because it is clear that error in the y component significantly depends on tuning parameter f, while it has low influence on the x component.

The proposed approximation has satisfying accuracy for modeling y component of magnetic flux density. The best value for tuning parameter is found by observing Fig. 8 and Fig. 10 as $f = 0.29$, for which error in y component is between -0.75% and $+0.02\%$ for the whole sag range. As a conclusion, the possible method for conductor sag estimation can be based only on y component of magnetic flux density of the proposed approximation, which is highly accurate and preserves information about real conductor sag.

As an illustration of the accuracy of the proposed model, instantaneous values of magnetic flux density vector components for real 20 kV overhead power line [9] are simulated for reference and approximate model, and are compared in Fig. 11. The sag of catenary is set to $s = 1$ m, span length is $L = 100$ m, while sag to span ratio is equal to $s/L = 1/100 = 0.01$. From Fig. 11b it can be concluded that the y component has very high level of accuracy compared to reference model, with error less than 1%.

However, since x and y components of magnetic flux model (22)–(23) are completely decoupled, some other procedure for calibrating the x component should be considered in order to obtain better accuracy, if needed. By this, different longitudinal tuning parameters f for x and y component can be selected.

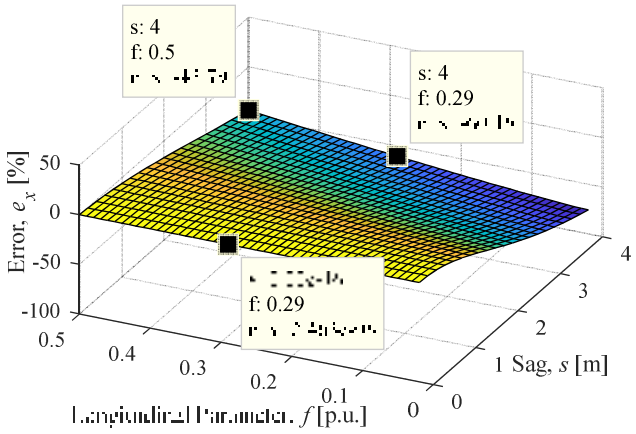

Figure 7. Error of approximate magnetic flux density x component

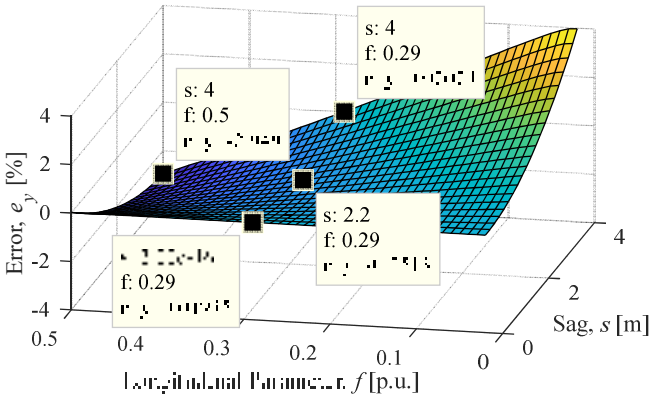

Figure 8. Error of approximate magnetic flux density y component

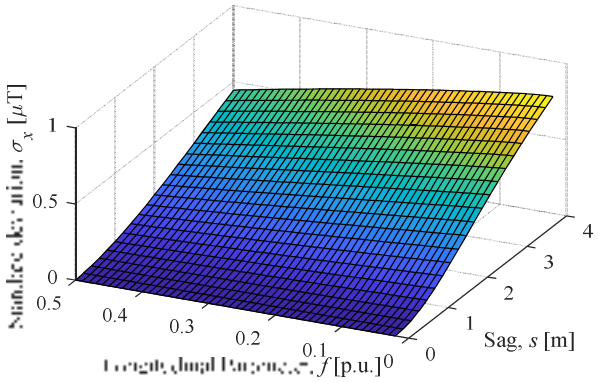

Figure 9. Standard deviation of $B_{x,approx.}$ component

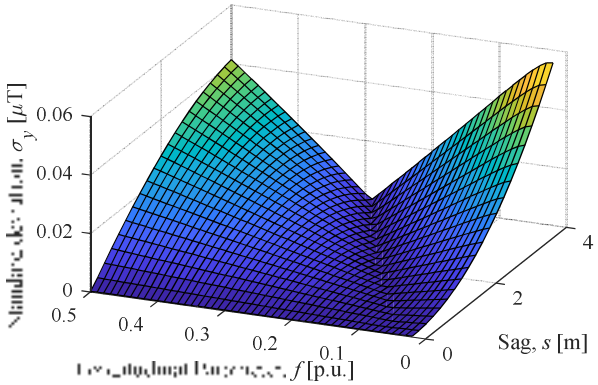

Figure 10. Standard deviation of $B_{y,approx.}$ component

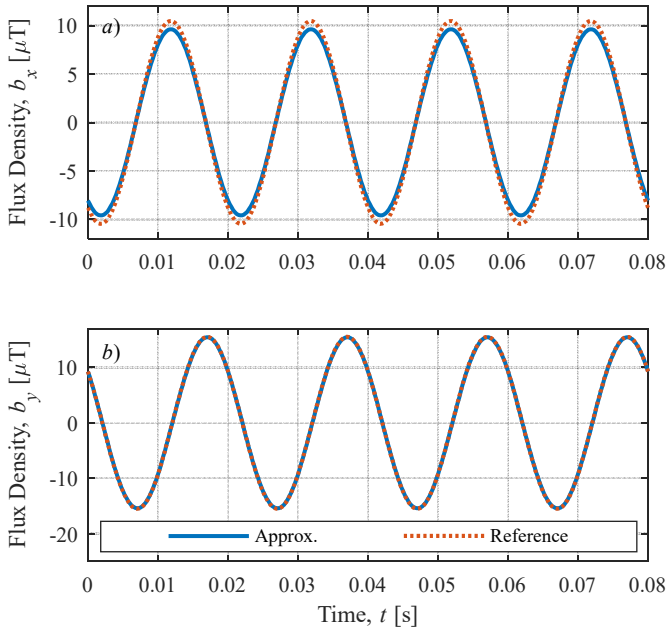

Figure 11. Magnetic flux density of approximate model (blue-solid) and reference model (red-dotted), for s=1 m, *a*) x and *b*) y component

V. Experimental Verification

Experimental verification of the accuracy of the proposed approximate magnetic flux density model is conducted on overhead power line model scaled for laboratory conditions, which is thoroughly described in [10]. The scaled power line model corresponds to the real 20 kV distribution overhead power line with geometry from Fig. 1. Power line model dimensions and currents are scaled based on principle of the magnetic flux density invariance. By this, the flux density of the scaled model is considered the same as for the real power line. Scaled model consists of two spans of the power line conductors, two angle poles with conductor tension regulation (Fig. 12) and one middle support pole with mounted magnetic flux density sensor and current measuring transformers (CMTs), for each phase conductor (Fig. 13a).

The magnetic flux density y component is measured by magnetic sensor (MS), while phase currents are measured by three single phase instrument CMTs, and the signals are processed through analog amplifying and filtering circuit [11]. Amplified and filtered signals are sampled with the Humusoft MF634 acquisition board, with sampling frequency of 2 kHz, and sampled signals are further digitally processed, as shown in Fig. 14.

In the experimental verification on the scaled laboratory model conductor sag is varied by changing the tension of the conductors and it is manually measured by a ruler placed at the middle of each span (Fig. 13b). The sag for the scaled model was in the range from $s_{min,scaled} = 0.03$ m to the $s_{max,scaled} = 0.16$ m on the scaled span length $L_{scaled} = 4$ m. The scaled sag range corresponds to the real catenary in range from $s_{min,real} = 0.75$ m to $s_{min,real} = 4$ m for the span length $L_{real} = 100$ m. Therefore, the sag to span ratio is identical for the scaled and real overhead power line, and ranges from $s_{min}/L = 0.0075$, to the $s_{max}/L = 0.04$.

Figure 12. Scaled angle pole with tension regulation

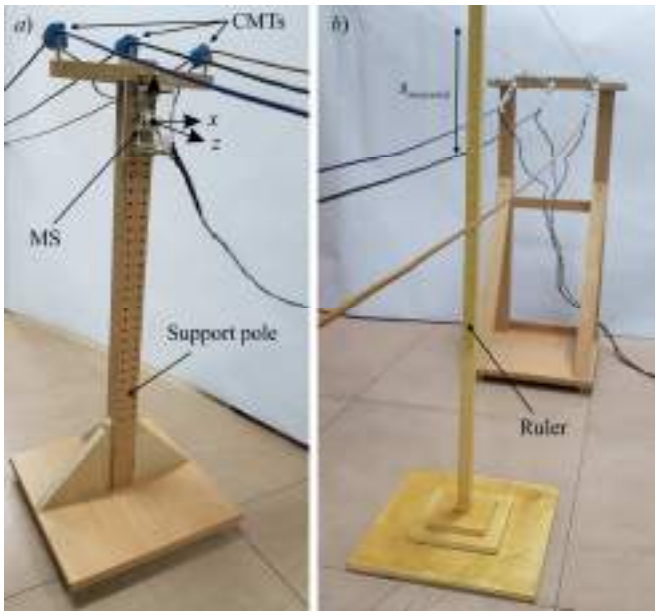

Figure 13. *a*) Support pole with MS and CMTs, *b*) Ruler for sag measurement

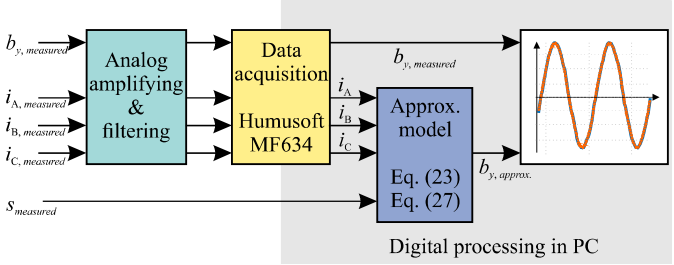

Figure 14. Data acquisition and processing

In order to verify the accuracy of the proposed model, measured instantaneous value of magnetic flux density y component is compared with value calculated from model (23) using measured sag and measured currents, as shown in Fig. 14. The results are shown in Fig. 15 and Fig. 16.

Fig. 15 shows magnetic flux density y component measured by MS and approximate magnetic flux density component calculated by employing model (23) using measured phase currents for $s/L = 0.0075$. From Fig. 15 almost complete match between approximate and measured magnetic flux density component is confirmed, as it is expected for low values of sag. In Fig. 16, the same signals are shown for very large sag to span ratio $s/L = 0.025$. Difference between approximate and measured y component signals is less than 2%, which confirms accuracy of the proposed model.

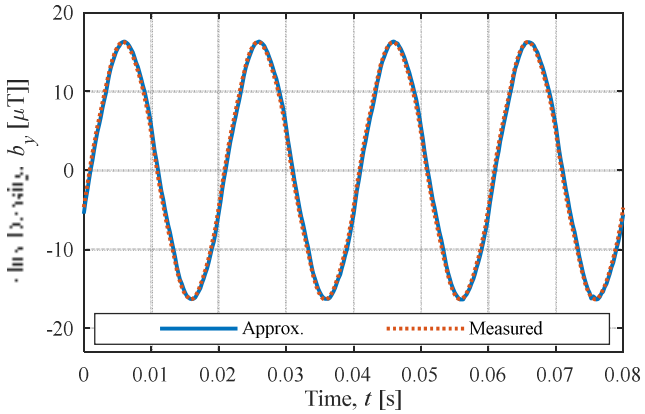

Figure 15. Magnetic flux density y component of approximate model (blue-solid) and measured (red-dotted) (s_{scaled} = 0.03 m, s_{real} = 0.75 m, s/L = 0.0075)

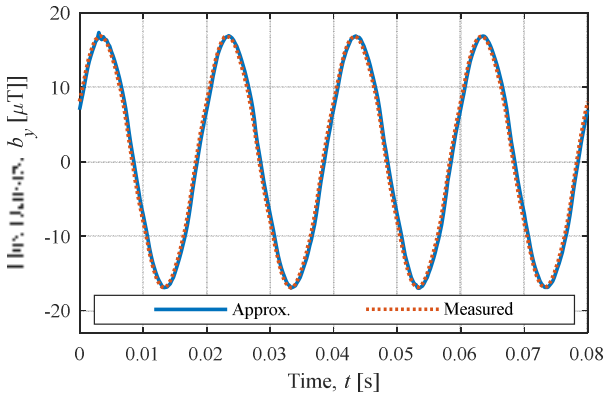

Figure 16. Magnetic flux density y component of approximate model (blue-solid) and measured (red-dotted) (s_{scaled} = 0.1 m, s_{real} = 2.5 m, s/L = 0.025)

VI. Conclusion And Future Work

In this paper an approximate magnetic flux density model of three-phase catenary-shaped overhead power line is proposed. The main property of the model is that the Biot-Savart line integral is solved in closed form by approximating catenary-shaped conductors with tilted straight half-lines. By proper calibration of the model, information about conductor sag is preserved, and the model is therefore applicable for power sag real-time line monitoring. The accuracy of the model is confirmed by computer simulations and experiments on the line model scaled to laboratory conditions. The proposed approach is applicable for arbitrary geometry of support pole, and both symmetrical and non-symmetrical operation of three-phase systems. Also, it can be expanded for modeling conductor sag in non-symmetrical line spans by using additional magnetic field sensors.

In further work, the proposed model of magnetic flux density will be used as a basis for real-time sag estimation by combining it with appropriate adaptive method (like Model Reference Adaptive System – MRAS) which will be added in Fig. 14 as a feedback using estimated sag in closed loop. By this, the model could be implemented as a software upgrade for online sag estimation in simple devices for power line monitoring, which already acquire information about magnetic field and phase currents for fault detection.

References

[1] X. Sun, Q. Huang, Y. Hou, L. Jiang, and P. W. T. Pong, "Noncontact Operation-State Monitoring Technology Based on Magnetic-Field Sensing for Overhead High-Voltage Transmission Lines," in *IEEE Trans. Power Del.*, vol. 28, no. 4, pp. 2145–2153, October 2013.

[2] Đ. Lekić, P. Mršić, B. Erceg, Č. Zeljković, N. Kitić and P. R. Matić, "Generalized Approach for Fault Detection in Medium Voltage Distribution Networks Based on Magnetic Field Measurement," in *IEEE Trans. Power Del.*, vol. 35, no. 3, pp. 1189 – 1199, June 2020.

[3] A. H. Khawaja, Q. Huang, J. Li and Z. Zhang, "Estimation of Current and Sag in Overhead Power Transmission Lines With Optimized Magnetic Field Sensor Array Placement," in *IEEE Trans. Magn.*, vol. 53, no. 5, pp. 1-10, May 2017.

[4] Ayman Uddin Mahin, Shama Naz Islam, Fabliha Ahmed, and Md. Farhad Hossain, "Measurement and Monitoring of Overhead Transmission Line Sag in Smart Grid: A review," in *IET Gener. Transm. Distrib.*, pp. 1– 18, August 2021.

[5] R. G. Olsen and K. S. Edwards, "A New Method for Real-Time Monitoring of High-Voltage Transmission-Line Conductor Sag," in *IEEE Trans. Power Del.*, vol. 17, no. 4, pp. 1142–1152, Oct. 2002.

[6] S. M. Mahajan and U. M. Singareddy, "A Real-Time Conductor Sag Measurement System Using a Differential GPS," in *IEEE Trans. Power Del.*, vol. 27, no. 2, pp. 475-480, April 2012.

[7] A. V. Mamishev, R. D. Nevels and B. D. Russell, "Effects of conductor sag on spatial distribution of power line magnetic field," in *IEEE Trans. Power Del.*, vol. 11, no. 3, pp. 1571-1576, July 1996.

[8] P. Patel, "Calculation of Total Inductance of a Straight Conductor of Finite Length," in *Phys. Educ.*, pp. 193–198, July − September 2009.

[9] Đ. Lekić, P. Mršić and Č. Zeljković, "Calculation of Magnetic Fields in the Vicinity of Overhead Transmission Lines for The Purpose of Fault Detection," in *Symposium Energy Efficiency – ENEF 2015*, Banja Luka, Republic of Srpska, pp. 58-63, 25-26 September 2015. (in Serbian)

[10] Đ. Lekić, P. Mršić, B. Erceg and Č. Zeljković, "Three Phase Line Model for Laboratory Testing of Fault Passage Indicators," in *The 10th Mediterranean Conference on Power Generation, Transmission, Distribution and Energy Conversion - Med Power 2016*, Belgrade, Serbia, pp. 1-8, 6-9 November 2016.

[11] Đ. Lekić, P. Mršić, B. Erceg, Č. Zeljković, N. Kitić and P. R. Matić, "Laboratory Setup for Fault Detection on Overhead Power Lines Based on Magnetic Field Measurement," in *International Symposium on Industrial Electronics and Applications – INDEL 2020*, Banja Luka, Republic of Srpska, 4-6 November 2020.

Nemanja Kitić (S'19) received the B.Sc. degree in Electrical Engineering from the University of Banja Luka, Republic of Srpska, Bosnia and Herzegovina in 2017, where he is employed as a teaching and research assistant. He is currently working toward the M.Sc. degree at the University of Banja Luka. His current research interests include sag estimation on overhead transmission lines, grounding systems and electrical machines and drives.

Petar R. Matić (M'13, SM' 17) received the B.Sc. and M.S. degree in Electrical Engineering from the University of Novi Sad, in 1999 and 2002, and Ph.D. degree from the Electrical Engineering Faculty, University of Belgrade, in 2011. He is an associate professor (2017-present) and Head of Department of Electrical Power Engineering, Faculty of Electrical Engineering, University of Banja Luka, Republic of Srpska, Bosnia and Herzegovina. His research area includes power engineering, electrical machines and electrical drives.